RAPID COMMUNICATIONS

PHYSICAL REVIEW B VOLUME 40, NUMBER 7 1 SEPTEMBER 1989

Strange attractors in parallel-pumped spin-wave instabilities: Bifurcation of multifractals

Michinobu Mino and Hitoshi Yamazaki
Department of Physics, Faculty of Science, Okayama University, Okayama 700, Japan

Katsuhiro Nakamura
The James Franck Institute, The University of Chicago, Chicago, Illinois 60637
*and Fukuoka Institute of Technology, Higashi-ku, Fukuoka 811-02, Japan**
(Received 12 May 1989)

An experimental study of strange attractors at and beyond the period-doubling accumulation point is made for parallel-pumped spin-wave instabilities in a ferrimagnetic yttrium iron garnet disk. Singularity spectra are found to show a distinctive bifurcation, in the transition region leading to the growth of a high-dimensional attractor. A microscopic theoretical model well explains this phenomenon.

Nonlinear spin-wave dynamics beyond the Suhl threshold is found to show rich structures of chaos and turbulence[1-8] comparable to those in fluid dynamics. The most attractive feature of the spin-wave instability would be that the microscopic interactions are well known. The microscopic theoretical model which includes the effect of a cavity mode explains a variety of experimental results (period-doubling cascade, quasiperiodicity, irregular relaxation oscillations, and chaos) very well.[8] To further compare experimental results with a theoretical model, detailed characterization of strange attractors is required. In this Rapid Communication, we shall present an experimental study of strange attractors at and beyond the period-doubling accumulation point for a parallel-pumped spin-wave instability in an yttrium iron garnet (YIG). In particular, the change in the multifractal structure of the strange attractor will be examined by increasing a driving power. Little attention has been given to a study of this kind so far. Though our major subject lies in an experimental aspect, some results of numerical iteration of the theoretical model will also be described.

Experiments were performed at a pumping frequency of 8.9 GHz at a temperature of 4.2 K. A disk-shaped YIG, 1.28 mm in diameter and 0.40 mm thick, is mounted on the bottom of the TE_{101} cavity. Both microwave and static fields are applied along the [111] direction perpendicular to the disk. Measurements were done in a field of 1935 G where the minimum threshold for instability is given by $P_{th}=0.3$ mW, which will be taken as $P_{th}=0$ dB in the following. The excited magnons have the wave number $k\sim 0$ and propagate perpendicularly to the static field. As the cavity is critically coupled, the spin-wave instability is detected in the reflected microwave power. Microwave signals are detected by a tunnel diode and recorded in a computer at intervals of 1 μsec.

Figure 1 shows power spectra and strange attractors which are constructed by the time delay method with a delay time of 3 μsec. An observed period-doubling cascade accumulates at $P=P_c=2.20$ dB, and developed chaotic oscillations whose power spectra exhibit broadbands are obtained at $P=2.97$ and 3.60 dB.

The singularity spectra $f(\alpha)$ are procured from whole trajectories embedded in five-dimensional space (each attractor has 20000 points). We first calculate the partition function $\Gamma(q,l)=\langle P_i(l)^{q-1}\rangle$, where the probability $P_i(l)$ is obtained by counting the number of points within the ith hyperspherical distribution with radius l and dividing it by the total number of points in the trajectory data set. The angular brackets represent an average over 2000 randomly chosen distributions. $\Gamma(q,l)$ has a wide scaling region satisfying $\Gamma(q,l)\sim l^{\tau(q)}$, which leads to $f(\alpha)$ with the use of the Legendre transformation.[9] Our experimental results have precisions up to the scale $l\sim 2^{-4}$, below

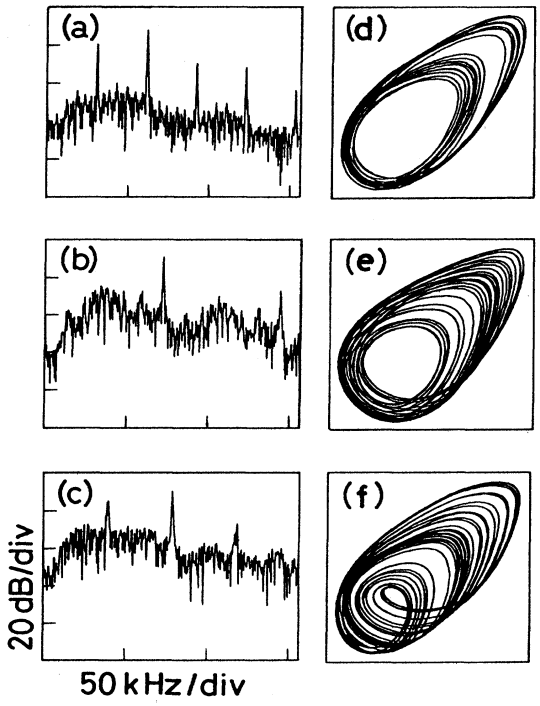

FIG. 1. Experimental result for power spectra (a)–(c), and strange attractors (d)–(f): (a),(d) $P=P_c=2.20$ dB; (b),(e) $P=2.97$ dB; (c),(f) $P=3.60$ dB.

which noise effects become operative. As the obtained $f(\alpha)$ spectra contain a trivial one dimension in the direction of trajectories, we hereafter subtract unity from both f and α.

The $f(\alpha)$ spectrum at $P=P_c=2.20$ dB is shown in Fig. 2(a). The maximum point of the curve (i.e., D_0) is 0.55 ± 0.04. This curve is consistent with the universal one for the period-doubling route[9] [see the solid curve in Fig. 2(a)]. At $P=2.97$ dB, however, $\Gamma(q,l)$ has two distinctly different scaling regions separated by a crossover region R_c [see Fig. 2(d)]. The scaling exponents $\tau(q)$ below and above R_c differ from each other. (Error bars associated with the individual scaling regions are too small to overcome the difference between these two exponents.) Consequently, there occur two kinds of coexisting humps or a "bifurcation" of $f(\alpha)$ [see Fig. 2(b)]. This bifurcation is due to the band structures of the strange attractors (i.e., island structures of their Poincaré section) emerging from the period-doubling route. In Fig. 2(b), the left-hand-side curve with $D_0=0.6$ is related to a larger-scale behavior (i.e., weak bunching which wanders with different bands), retaining a feature of the universal curve at the critical point. The right-hand curve with $D_0=1.0$ is related to a small-scale curve (i.e., strong bunching in each band), describing a new multifractal structure. [The scales of both abscissas and ordinates in Figs. 2(b) and 2(c) differ from the ones in Fig. 2(a).] At $P=3.60$ dB, a unique $\tau(q)$ is recovered. The $f(\alpha)$ curve in Fig. 2(c) has a fractal dimension of $D_0=1.0$. By increasing the power further, the oscillations become periodic again and exhibit period halving. Period 4, period 2, and period 1 are observed at $P=4.08$, 4.32, and 5.25 dB, respectively. A further increase of driving power causes the growth of higher-dimensional attractors. The correlation dimensions D_2, which are obtained with use of a correlation integral, are 1.4, 2.0, 2.4, and 3.2 at $P=8.56$, 13.01, 14.73, and 16.20 dB, respectively. Thus, the bifurcation of $f(\alpha)$ is followed by the growth of high-dimensional attractors. Note: In both Figs. 2(b) (right-hand-side curve) and 2(c), the $f(\alpha)$'s cannot be attributed to the quasiperiodic origin because the Poincaré sections of the attractors in Fig. 1 indicates no torus structure characteristic of quasiperiodic attractors. In general, we cannot expect this kind of bifurcation in the case of the quasiperiodic route to chaos,[10] because the trajectory at its criticality shows no band structure.

To stimulate the present system, we employ a theoretical model with four-magnon interaction as shown in Fig. 3. The equation of motion for spin-wave modes C_k $(=C_{-k})$ is

$$\dot{C}_k=-\gamma_k C_k-i\Delta\Omega_k C_k-iQFg_k C_k^*-i\left[2\sum_{k'}T_{kk'}|C_{k'}|^2C_k+\sum_{k'}(S_{kk'}+Eg_kg_{k'}^*)C_{k'}^2C_{k'}^*\right], \tag{1}$$

where γ_k, $\Delta\Omega_k$, g_k, and $F(\equiv h_pV)$ are damping constants for C_k, frequency shifts, coupling between the cavity mode and C_k, and a driving field, respectively. $T_{kk'}$ and $S_{kk'}$ denote the coupling among spin waves. Equation (1) is formally identical to the equation employed in the case of the first-order perpendicular pumping.[8] However, in our parallel pumping case a cavity mode couples directly with spin-wave pairs, thereby producing new expressions for Q and E: $Q=-i/\Gamma$ and $E=-i/(2\Gamma)$, with Γ being the damping constant for the cavity mode. Further, in marked contrast to Ref. 8, g_k are vanishing for the mode propagating parallel to a static field. We now confine to the case of two modes a system where $g_{k1}\neq0$ and $g_{k2}=0$. Noting the realistic parameter values in Ref. 11, we take $\hat{F}=F\times10^7\ \mathrm{sec}^{-1}$ in the following: Consistent with experimental results, a period-doubling cascade accumulates at the critical point $\hat{F}=\hat{F}_c=1.92286$. When $\hat{F}$ is increased beyond $\hat{F}_c$, we see a gradual growth of a higher-dimensional strange attractor. Some aspects of this dramatic change in the attractor may also be described on the basis of a unique low-dimensional map, e.g., a Henon

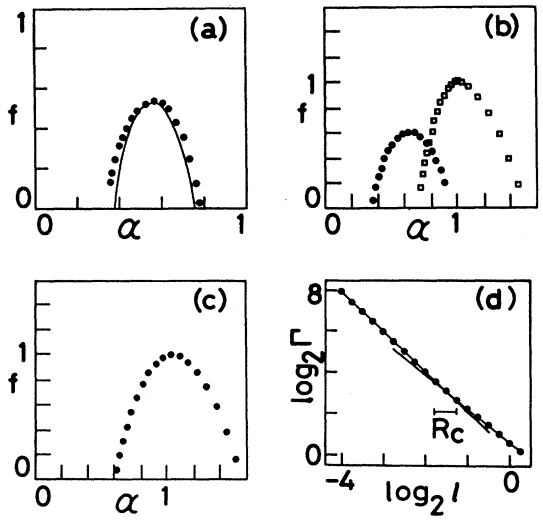

FIG. 2. Experimental $f(\alpha)$ spectra: (a) $P=2.20$ dB; (b) $P=2.97$ dB; (c) $P=3.60$ dB. (d) Experimental $\Gamma(q,l)$ in logarithmic scales at $P=2.97$ dB ($q=0$).

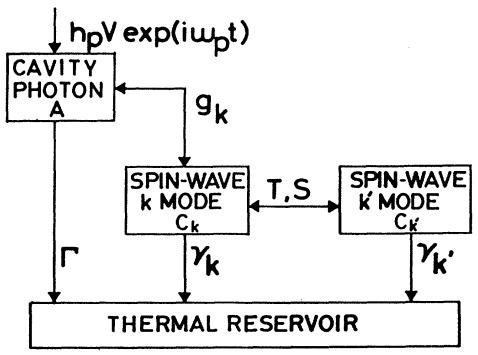

FIG. 3. Theoretical mechanism behind Eq. (1).

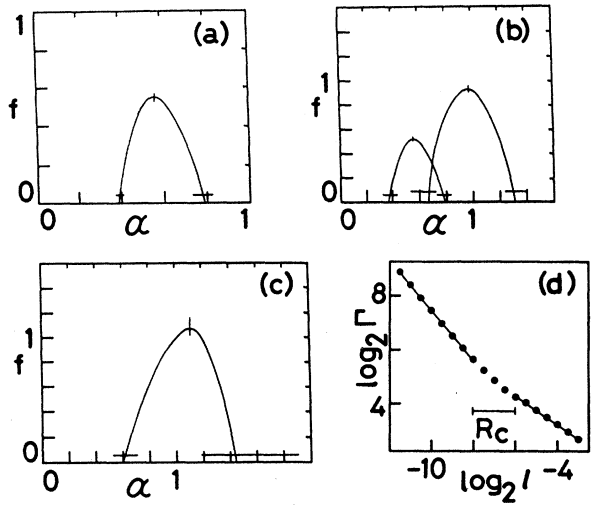

FIG. 4. Computed $f(\alpha)$ spectra of Eq. (1): (a) $\hat{F}=\hat{F}_c=1.92286$; (b) $\hat{F}=1.9229$; (c) $\hat{F}=1.94$. (d) Computed $\Gamma(q,l)$ in logarithmic scales at $\hat{F}=1.9229$ ($q=0$).

map. Our microscopic model has a greater advantage, however, because it is directly related to a set of microscopic material constants of YIG. The singularity spectra $f(\alpha)$ are calculated here by using the Poincaré sections of the attractors. (We have obtained 8000 points for each section.)

The $f(\alpha)$ curve at $\hat{F}=\hat{F}_c$ in Fig. 4(a) is almost identical to the universal one. The accuracy of D_0, $\alpha_{\max}$, and $\alpha_{\min}$ is indicated by error bars. At $\hat{F}=1.9229$, $\Gamma(q,l)$ has a crossover region R_c [see Fig. 4(d) and note that a noise level lies only in the region $l \leqq 2^{-12}$], and "bifurcation" of $f(\alpha)$ is observed [see Fig. 4(b)], which is quite similar to the experimental issue in Fig. 2(b). When $\hat{F}$ increases further, R_c moves toward a larger scale region, and finally at $\hat{F}=1.94$ in Fig. 4(c), we find no indication of a crossover region. Corresponding D_0 are 0.54 and 1.07 at $\hat{F}=\hat{F}_c$ and 1.94, respectively, while we have two D_0 values, 0.51 and 0.92, at $\hat{F}=1.9229$. [A one-mode model here can, of course, yield no chaotic attractor and the two-mode model proves enough to describe the bifurcation of $f(\alpha)$.] Furthermore, we have obtained $D_0=1.8$ at $\hat{F}=2.20$. Much larger values of D_0 will be available by increasing the number of active spin-wave modes. The theoretical model thus explains most of our experimental issues very well.

In conclusion, our experiments indicate a route toward a high-dimensional attractor via the transition region where $f(\alpha)$ shows a remarkable bifurcation. A microscopic theoretical model captures the essential aspect of this phenomenon.

One of us (K.N.) is grateful to A. Libchaber and S. A. Rice for fruitful discussions at the University of Chicago.

*Permanent address.

[1]K. Nakamura, S. Ohta, and K. Kawasaki, J. Phys. C **15**, L143 (1982); S. Ohta and K. Nakamura, *ibid.* **16**, L605 (1983).

[2]G. Gibson and C. Jeffries, Phys. Rev. A **29**, 811 (1984).

[3]X. Y. Zhang and H. Suhl, Phys. Rev. A **32**, 2530 (1985); Phys. Rev. B **38**, 4893 (1988).

[4]F. M. de Aguiar and S. M. Rezende, Phys. Rev. Lett. **56**, 1070 (1986); S. M. Rezende, O. F. de Alcantra Bonfim, and F. M. de Aguiar, Phys. Rev. B **33**, 5153 (1986).

[5]M. Mino and H. Yamazaki, J. Phys. Soc. Jpn. **55**, 4168 (1986).

[6]H. Yamazaki and M. Warden, J. Phys. Soc. Jpn. **55**, 4477 (1986); H. Yamazaki, M. Mino, H. Nagashima, and M. Warden, *ibid.* **56**, 742 (1987).

[7]T. Carroll, F. Rachford, and L. Pecora, Phys. Rev. B **38**, 2938 (1988).

[8]P. Bryant, C. Jeffries, and K. Nakamura, Phys. Rev. Lett. **60**, 1185 (1988); Phys. Rev. A **38**, 4223 (1988).

[9]T. Halsey, M. Jensen, L. Kadanoff, I. Procaccia, and B. Shraiman, Phys. Rev. A **33**, 1141 (1986).

[10]J. Glazier and A. Libchaber, IEEE Trans. Circuits Syst. **35**, 790 (1988).

[11]Parameter values used in the present text are as follows: $g_{k1}=0.2i\times10^6$, $g_{k2}=0$, $\Gamma=1.0\times10^8$, $\gamma_{k1}=0.1\times10^5$, $\gamma_{k2}=0.2\times10^5$, $T_{11}=-0.5\times10^{-8}$, $T_{22}=0.25\times10^{-8}$, $T_{12}=T_{21}=2.0\times10^{-8}$, $S_{11}=-0.5\times10^{-8}$, $S_{22}=0.25\times10^{-8}$, $S_{12}=S_{21}=4.5\times10^{-8}$, $\Delta\Omega_1=\Delta\Omega_2=0$ ($\sec^{-1}$).